MODES OF DECOMPOSITION OF RARE EARTH METAL FORMATES AND BENZOATES, ENTHALPIES OF TRANSITION, AND ACTIVATION ENERGIES OF DECOMPOSITION

M. D. TAYLOR and R. PANAYAPPAN*

Department of Chemistry, Howard University Washington, D. C. 20001 U.S.A.

(Received February 15, 1973)

The modes of decomposition of a few rare earth metal formates and benzoates were studied by the use of DTA, DSC, TG and DTG techniques in air, nitrogen and vacuum. The volatile products and residues were identified. The activation energies of decompositions and the heat of reaction for transitions were calculated.

The decomposition of the rare earth metal formates gave carbon dioxide and water as their volatile products and the benzoates gave benzil and probably benzophenone in the case of lanthanum benzoate and biphenyl in the case of other rare earth metal benzoates, as their main volatile products, leaving the corresponding trioxides as their final residues.

Although the formates of rare earth metals have been prepared by a number of workers [1−5], the systematic study of their thermal decomposition has not been done. Deshpande and Mizra [4] have studied the decomposition in air and nitrogen but not in vacuum. We have studied the thermal behavior of the formates in air, nitrogen and vacuum. We have also prepared and studied some rare earth metal benzoates under the same conditions. This paper describes the mode of decomposition of these compounds in different media, gives the heat of reaction for phase transitions of rare earth metal benzoates, and the activation energies for the decomposition of formates and benzoates.

Considerable interest exists in the study of changes which occur in solid inorganic compounds as they are uniformly heated. By studying such changes much information can be gained concerning the mode of decomposition, phase changes, energies of transition, heats of decomposition and similar properties. Also one often discovers novel methods of preparing compounds.

In this study we have examined the thermal behaviour of rare earth metal formates and benzoates by differential scanning, differential thermal and thermogravimetric techniques. The differential scanning technique yielded information which enabled us to identify transitions and compute enthalpies of transition. The thermogravimetric technique enabled us to determine modes of decomposition and compute activation energies.

Experimental

Starting materials. The source of the lanthanide materials was lanthanide oxides 99.99 percent pure. They were purchased either from Research Chemicals, Inc., Burbank, California, or Lindsay Chemical Division, West Chicago, Illinois. Formic acid and sodium benzoates were reagent grade.

Preparation. All the formates were prepared by the method described by Ambrozhii and Osipova [6]. The rare earth metal benzoates were prepared by the method published by Taylor, Carter and Wynter [7].

Apparatus and procedure. Measurements were made with the Du Pont Differential Thermal Analyzer (DTA), differential scanning calorimeter (DSC), models 900 and 990, and the thermogravimetric analyser (TGA), models 950 and 951. The TGA, model 951, possesses derivative thermogravimetric (DTG) capability. The infrared 621 Perkin—Elmer spectrophotometer was used for obtaining IR spectra of TG residues and volatile products. A Coleman-33 carbon hydrogen analyzer was used for the determination of carbon and hydrogen.

Differential thermal studies were performed by placing about 3.0 mg of the sample in a quartz tube, 4.0 mm deep. Alumina was used as the reference. In all cases the thermocouples were immersed inside the sample and reference.

Differential scanning studies were performed by placing 5.0 to 15.0 mg of the sample in an aluminum sample pan and using an empty aluminum pan for a reference. Both pans were covered by a bell Jar which permitted the use of various atmospheres. Data for thermal curves were plotted as Δqs (the difference between the heat energy absorbed by the sample and reference) versus temperature or time as required.

Thermogravimetric analysis was performed on 5.0 to 20.0 mg samples in various atmospheres usually at a heating rate of 20°/min. The TG results were plotted as weight lost against temperature. DTG curves were obtained as the rate of weight lost against temperature.

The sample holder was a small platinum boat (about 0.5 cm in depth), opened at both ends, attached to a quartz rod. The thermocouple was adjacent to the boat but not touching it. The samples were loaded by means of a microspatula. A stream of dry air, ultrapure nitrogen or CO_2 was passed around the samples.

Results and discussion

Rare earth metal formates

The composition of the formates was verified by analysis for carbon and hydrogen. The data for the analyses are given in Table 1. In most cases the experimental result approximates closely the values required by theory. The agreement for $Sm(OOCH)_3$ is poor but the thermogravimetric analytical data indicated a pure compound. The benzoates were analyzed in a similar manner. The data are given in Table 2 where again the agreement is seen to be quite good.

Differential thermal analysis

DTA data obtained for the formates of La, Sm, Eu, Tb and Er are summarized in Table 3. The formates of La, Sm and Er exhibited a broad endothermic transition in the vicinity of 160°. Eu and Tb formates exhibited a sharp exothermic

Table 1

Carbon-hydrogen analysis of rare earth metal formates

Compound	% carbon		% hydrogen	
	found	calc.	found	calc.
$La(OOCH)_3$	13.2	13.1	1.13	1.10
$Sm(OOCH)_3$	13.3	12.9	1.07	1.19
$Eu(OOCH)_3$	12.1	12.6	1.28	1.05
$Tb(OOCH)_3$	12.1	12.2	1.05	1.02
$Er(OOCH)_3$	11.9	11.9	0.99	0.99

Table 2

Carbon-hydrogen analysis of rare earth metal benzoates

Compound	% carbon		% hydrogen	
	found	calc.	found	calc.
$La(BZ)_3$*	49.90	50.20	3.19	2.98
$Nd(BZ)_3$	49.36	49.96	3.04	2.96
$Eu(BZ)_3$	48.87	48.93	2.83	2.90
$Tb(BZ)_3$	48.40	48.28	2.91	2.87
$Er(BZ)_3$	47.87	47.53	2.98	2.83

* $BZ = C_6H_5CO_2^-$

Table 3

DTA data for rare earth metal formates in air (Temperature, °C)

$La(OOCH)_3$	$Sm(OOCH)_3$	$Eu(OOCH)_3$	$Tb(OOCH)_3$	$Er(OOCH)_3$
160−200, Endo (b)	155−195, Endo (b)	—	—	130−170, Endo (b)
—	—	275, Exo (sp)	265, Exo (s, sp)	—
420, Endo (s, sp), d	420, Endo (s, sp), d	405, Endo (s, sp), d	405, Endo (s, sp), d	310, Endo (s, sp) (d)
450, Endo (m, sp)	—	455, Endo (w, sp)	—	345, Endo (w)
				380, Endo (w)
770, Endo (sp)	749, Endo (s, sp)	720, Endo (w)	715, Endo (m, b)	500, Exo (m)

b = broad, d = decomposition, m = medium, s = strong, sp = sharp, w = weak

transition in the neighborhood of 270°. All compounds, except Er formate, started decomposing above 400°, the latter started decomposing above 300°.

The decomposition product appears to be a basic carbonate. The decomposition temperatures appear to decrease with increasing atomic number of the metal. The final decomposition occurred above 700° and was endothermic. The final decomposition temperature of Er formate, which exhibited an exothermic peak at 500°, was indefinite.

Thermogravimetric analysis

Thermogravimetric analyses data obtained for the same compounds are summarized in Table 4. The symbols are defined as follows: T_i is for the temperature of inception, T_s for the temperature at which the reaction is maximum and T_f for the temperature at which the reaction ends. In most cases the decomposition occurred in two stages in accordance with the equation
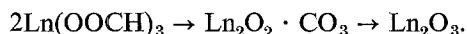
$$2Ln(OOCH)_3 \rightarrow Ln_2O_2 \cdot CO_3 \rightarrow Ln_2O_3.$$

Table 4

Procedural decomposition temperatures (°C) for rare earth metal formates

Compound	1st stage			2nd stage		
	T_i	T_s	T_f	T_i	T_s	T_f
La(OOCH)₃						
Vacuum	350	400	450	—	—	950
N₂	310	395	470	670	740	780
Air	350	430	480	740	815	880
Sm(OOCH)₃						
Vacuum	310	440	480	—	—	700
N₂	280	420	480	600	680	720
Air	305	420	470	650	690	740
Eu(OOCH)₃						
Vacuum	320	380	440	—	—	700
N₂	310	405	470	530	590	690
Air	310	390	405	610	650	680
Tb(OOCH)₃						
Vacuum	380	445	560	—	—	880
N₂	210	420	460	540	610	660
Air	320	410	430	535	565	600
Er(OOCH)₃						
Vacuum	280	360	420	—	—	950
N₂	230	315	370	—	—	920
Air	280	350	400	590	—	650

The DTA data for the lanthanide formates (Table 3) indicate a more complex mode of decomposition than the one shown above. A monoxycarbonate, $Ln_2O(CO_3)_2$, may be formed in the case of $Eu(OOCH)_3$ and $Tb(OOCH)_3$, as has been suggested by Kavadia and Mathur [5].
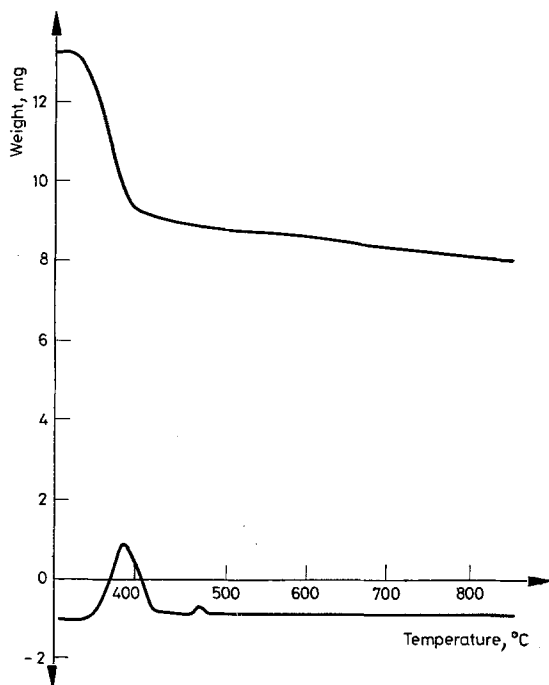

Fig. 1. TG and DTG curves of lanthanum formate in vacuum

Data in Table 4 indicate that the oxycarbonates usually decompose below 950°. However, the dioxycarbonate can exist at temperatures higher than 1000°, in an atmosphere of CO_2.

Observation of Table 4 indicates no appreciable variation in decomposition temperatures with the nature of the medium for the first stage of decomposition, except in nitrogen where the decomposition temperatures were usually slightly lower. In vacuum no clear cut indication of the second stage decomposition was obtained other than the final decomposition temperatures.

The second stage of the decomposition, just as the first stage, showed very little variation of decomposition temperature with the nature of the media. In general the characteristic temperatures appear to decrease with increasing atomic number but there are exceptions.

Table 5

Data for the composition of the decomposition products of rare earth metal formates

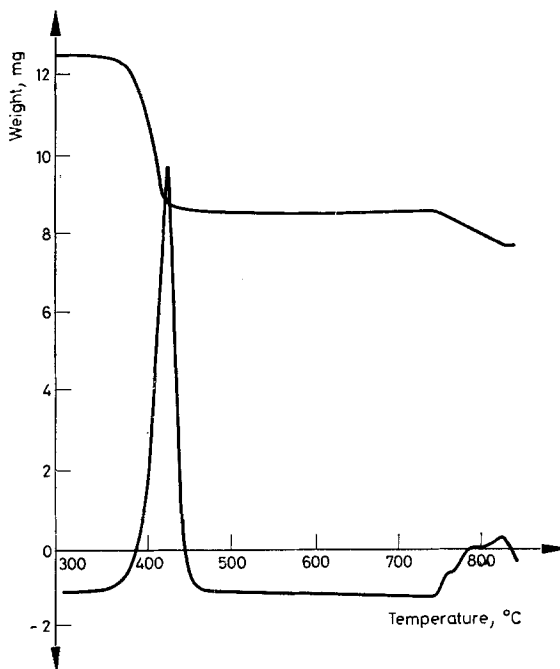| Compound	Wt. of sample		Mole wt. of first residue		Mole wt. of second residue	
	mg	mmole	Exp.	Calc.*	Exp.	Calc.
$La(OOCH)_3$	13.9	0.0507	186.4	185.0	163.7	163
$Sm(OOCH)_3$	12.0	0.0420	193.0	196.0	175.8	174
$Eu(OOCH)_3$	10.8	0.0376	199.6	198.0	171.0	176
$Tb(OOCH)_3$	11.65	0.0396	202	205	188	187 (Tb_4O_7)
$Er(OOCH)_3$	13.8	0.0457	210.2	213	192.6	191.0

* Assuming $1/2\ Ln_2O_2CO_3$.

Fig. 2. TG and DTG curves of lanthanum formate in air

Some typical thermal curves for the decomposition of rare earth metal formates are given in Figs 1, 2, 3 and 4. Data supporting the mode of decomposition are recorded in Table 5. One sees that the agreement between the experimental results and the calculated results is quite good.
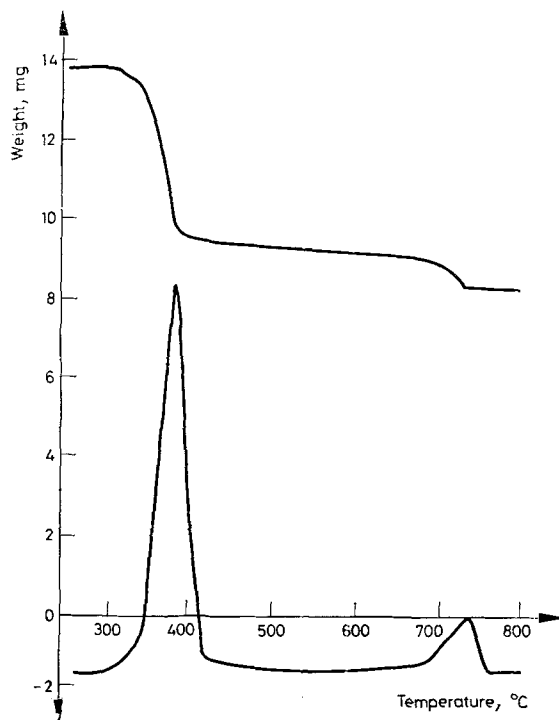
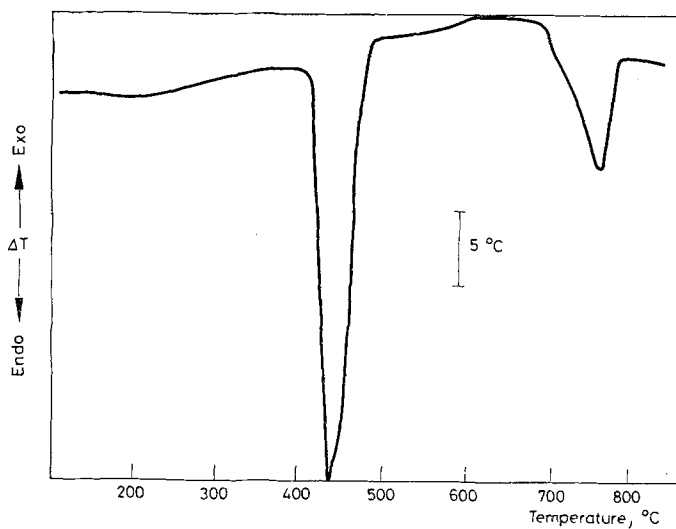Fig. 3. TG and DTG curves of lanthanum formate in nitrogen

Fig. 4. DTA curves of samarium formate in air

In addition to mole weight, infrared spectra were also used to identify the decomposition products of neodymium formate.

Infrared spectral data are listed in Tables 6 and 7. The band agreement supports the identification of the compounds. The bands observed agree with the bands reported by Goldsmith and Ross [9] for neodymium oxycarbonate. The final decomposition product, Nd_2O_3, yielded the infrared bands 675, 410 and 235 cm^{-1}. Goldsmith and Ross gave the bands 440, 320 and 285 cm^{-1} and McDevitt and Baun [10] listed the band, 655 cm^{-1}.

Activation energies

The activation energies for these decompositions were calculated by the method of Horowitz and Metzger [11] with the modification given by Dharwadkar and Karkhanavala [12]. The equation used for the calculation is:

$$E_a = \text{Slope} \cdot \frac{T_f - T_i}{100} RT_i^2 \quad (T = \text{degrees Kelvin})$$

A typical slope obtained by plotting $\ln \ln \dfrac{W - W_f^t}{W_0 - W_f^t}$ vs. Θ is given in Fig. 5. Here $\Theta = T - T_s$, W = weight remaining at a given temperature, W_0 = initial weight and W_f^t is the final weight for that particular decomposition step. Obtaining the slope by actually plotting the data proved rather tedious. It was more conveniently obtained with the use of a computer programme written with the help of Professor Elton Price of the Chemistry Department and Mr. Charles Moore of the Computer Center.
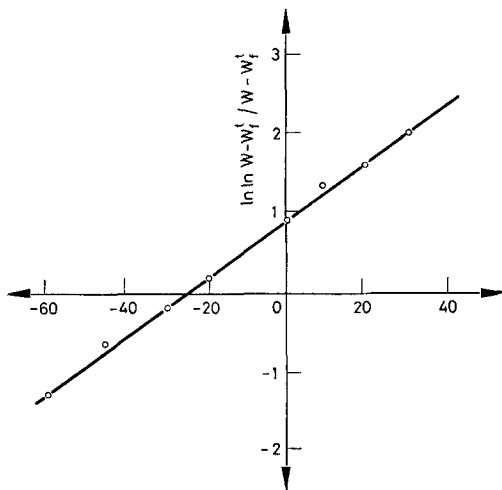

Fig. 5. Typical $\ln \ln \dfrac{W - W_i^t}{W_0 - W_f^t}$ vs. Θ plots

Table 8 gives the activation energies calculated for the first step of decomposition in air, nitrogen and vacuum. The activation energies appear to decrease with increasing atomic number in air and nitrogen, except for terbium. The values in

Table 6

Data for infrared spectrum of neodymium formate

Frequencies in cm^{-1}		Band assignment [8]
Observed	Reported [8]	
2945	2930	C—H stretch
1570—1610	1587	Asym. C—O stretch
1440	1401	In-plane C—H bend
1352	1353	Sym. C—O stretch
1080	1080	Out of plane C—H bend
780	783	Sym. C—O bend

Table 7

Data for the infrared spectrum of the intermediate decomposition product of neodymium formate

Frequencies in cm^{-1}		Band assignment [9]
Observed	Reported for Nd$_2$O$_2$CO$_3$ [9]	
1460	1470	
1365	1365	Assymmetric stretching
1060	1060	Symmetric stretching
830	830	Out of plane bending
350—390 (bd)	360 (bd)	

Table 8

Activation energy data for the decomposition of rare earth metal formates

Compound	Activation energies (kcal/mole) in		
	air	nitrogen	vacuum
La(OOCH)$_3$	67.3	59.3	32.1
	68.6	60.1	
Sm(OOCH)$_3$	44.9	38.6	36.6
Eu(OOCH)$_3$	39.4	43.3	—
Tb(OOCH)$_3$	49.6	37.0	45.2
Er(OOCH)$_3$	33.4	29.5	36.0

vacuum are essentially the same with terbium deviating from the trend. The stability for the rare earth formate appears to decrease with increasing atomic number. Data for the second step of decomposition were not suitable for the calculation of activation energies.

Rare earth metal benzoates

Elemental analyses for carbon and hydrogen have been given in Table 2.

Differential thermal analyses

Differential thermal analytical data were obtained for the benzoates of La, Nd, Eu, Tb and Er. These data are summarized in Table 9. All these benzoates except erbium exhibited a sharp endothermic peak in the neighborhood of 250°, erbium benzoate exhibited the transition at 290°. The first endothermic transition was reversible in all cases. However the cooling exotherm was not identical to the heating endotherm; these two temperatures approached each other more closely as the rate of cooling decreased, but as expected, never became identical. These peaks apparently represent transition temperatures. The final decomposition occurring around 600° was endothermic.

Table 9

DTA temperatures (°C) for rare earth metal benzoates in air

Lanthanum	Neodymium	Europium	Terbium	Erbium
245, Endo (w, sp)	240, Endo (m, sp)	250, Endo (w, sp)	235, 250, Endo (s, sp)	290, Endo (m, sp)
565, Endo (w, b)	580, Endo (m, sp)	545, 555, Endo (m, sp)	570, Endo (s, sp)	—
620, Endo (w)	590, Endo (m, sp)	—	500, Endo (w, sp)	590, Endo (s, sp)
630, Endo (w, sp)	—	—	—	618, Endo (s, sp)

b = broad, m = medium, s = strong, sp = sharp, w = weak

Differential scanning calorimetry

Differential scanning calorimetric data of the first transition for La, Nd, Eu, Tb and Er benzoates were obtained. Observe that the DSC temperatures are quite close to the DTA temperatures listed in Table 9. The values of ΔH (kcal/mole) and the transition temperatures are summarized in Table 10.

The values for ΔH are calculated using the equation given in the Du Pont 990

instruction manual [13]. The basic equation is ΔH (mcal/mg) $= \dfrac{A}{m}$ (60 $BE\Delta q_s$),

where A = peak area (sq. in.), m = sample mass (mg), B = time base setting (min/inch), E = cell calibration coefficient at the temperature of transition (dimensionless) and Δq_s = Y axis range (mcal/sec/in). The quantity (60 $BE\Delta q_s$) in

Table 10

Differential scanning calorimetric data
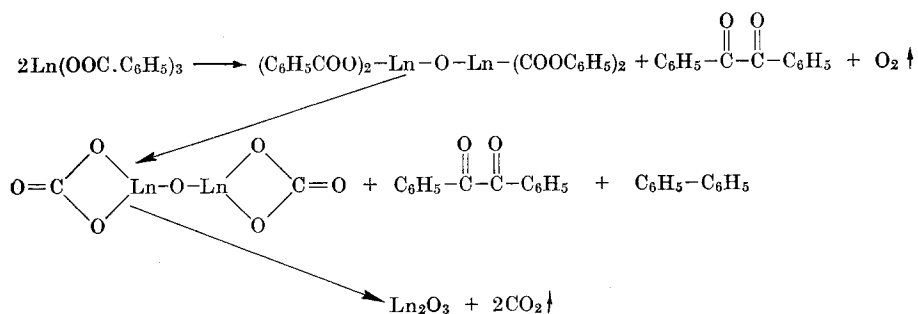for the rare earth metal benzoates

Compound	Transition temp., °C	ΔH (kcal/mole)
La(OOC · C$_6$H$_5$)$_3$	252	4.4
Nd(OOC · C$_6$H$_5$)$_3$	240	8.7
Eu(OOC · C$_6$H$_5$)$_3$	247	11.7
Tb(OOC · C$_6$H$_5$)$_3$	250	12.9
Er(OOC · C$_6$H$_5$)$_3$	285	12.6

mcal/sq. in. is constant for any given set of instrument settings. It can be used to convert area directly into heats of reaction.

From Table 10 it is seen that the heat of transition gradually increases as the atomic number increases.

Thermogravimetric analysis

Thermogravimetric analysis data were obtained for these same compounds. The results are summarized in Table 11 and 12. In most cases the decomposition occurred in three stages in accordance with the equation,

$$2Ln(OOC.C_6H_5)_3 \longrightarrow (C_6H_5COO)_2-Ln-O-Ln-(COOC_6H_5)_2 + C_6H_5-\overset{O}{\overset{\|}{C}}-\overset{O}{\overset{\|}{C}}-C_6H_5 + O_2\uparrow$$

Support for this mechanism is given by the data in Tables 11 and 12. Procedural decomposition temperatures in Table 11 support a three step mechanism and mole weight data in Table 12 support the decomposition products postulated.

DSC, TG and DTG curves obtained for neodymium benzoate are given in Figs 6 and 7. The three steps mode of decomposition is clearly indicated in the TG curve in Fig. 7.
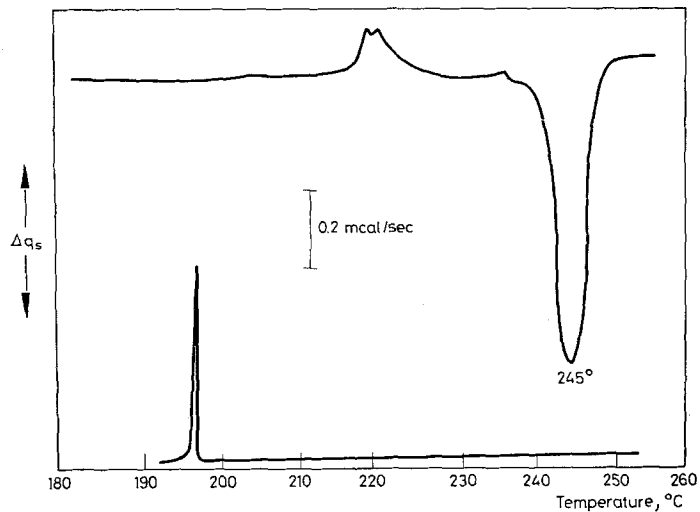

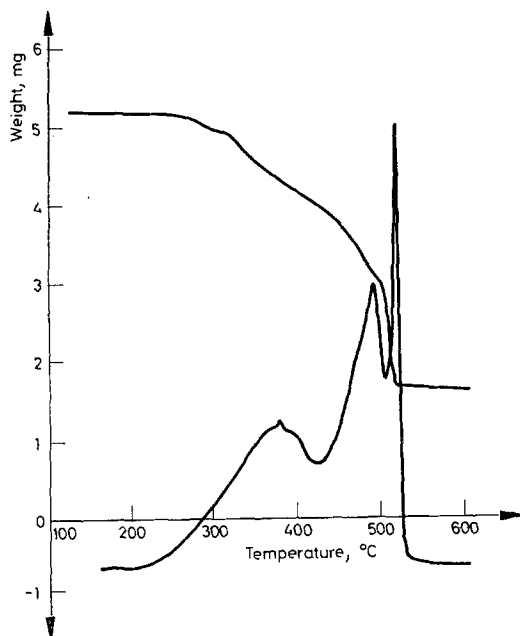Fig. 6. DSC curves (heating and cooling) of neodymium benzoate in air

Fig. 7. TG and DTG curves of neodymium benzoate in vacuum

Table 11

Procedural decomposition temperatures (°C) for rare earth metal benzoates

Compound	1st stage			2nd stage			3rd stage		
	T_i	T_s	T_f	T_i	T_s	T_f	T_i	T_s	T_f
La(COOC$_6$H$_5$)$_3$									
Vacuum	250	390	450	460	530	550	550	—	650
N$_2$	—	—	—	440	515	580	580	615	(720)
Air	300	340	370	470	495	510	765	785	810
Nd(COOC$_6$H$_5$)$_3$									
Vacuum	220	365	415	415	485	505	505	507	510
N$_2$	—	—	—	350	570, 585	(620)	—	—	—
Air	235	320	370	370	430	465	470	490	500
Eu(COOC$_6$H$_5$)$_3$									
Vacuum	220	320	380	380	420	465	465	490	510
N$_2$	—	—	—	330	550, 585	(610)	—	—	—
Air	300	—	—	410	445	450	—	—	610
Tb(COOC$_6$H$_5$)$_3$									
Vacuum	240	400	450	450	510	520	—	—	520
N$_2$	—	—	—	380	540, 580	(640)	—	—	—
Air	280	—	—	—	—	—	460	500	520
Er(COOC$_6$H$_5$)$_3$									
Vacuum	260	400	465	465	550	(610)	—	—	—
N$_2$	—	—	—	320	560, 570	640	—	—	—
Air	250	330	450	450	470	490	490	510	520

Table 12

Data for the composition of the decomposition products of rare earth metal benzoates in vacuum

Compound	Wt. of samples		Mole wt. of first residue		Mole wt. of second residue		Mole wt. of third residue	
	mg	mmoles	exp.	calc.	exp.	calc.	exp.	calc.
La(C$_6$H$_5$COO)$_3$	14.9	0.0297	390.5	389	186.8	185+	167	163
Nd(C$_6$H$_5$COO)$_3$	5.0	0.00986	395.5	394	213	212*	172	168
Eu(C$_6$H$_5$COO)$_3$	16.8	0.0327	—	—	—	—	174.3	174
Tb(C$_6$H$_5$COO)$_3$	5.6	0.01073	—	—	—	—	184	180 (Tb$_4$O$_7$)
Er(C$_6$H$_5$COO)$_3$	5.6	0.01060	—	—	—	—	196	191

+ 1/2 La$_2$O$_2$CO$_3$
* 1/2 Ln$_2$O(CO$_3$)$_2$

Further support for the mode of decomposition proposed was obtained by analysing the volatile decomposition product coming out of the furnace. This product condensed as yellow needles which melted at $94-95°$, the melting point of benzil. An infrared spectrum of the compound also proved to be identical with that of benzil.

By holding the temperature at $420°$ it was possible to isolate the first decomposition product which proved to be benzil. By heating the residue to a higher temperature a second decomposition product was obtained which proved to be benzil also. We were unable to isolate the product assumed to be biphenyl.

The examination of Table 11 reveals no appreciable variation in decomposition temperatures in vacuum and air except for La and Eu benzoates. In nitrogen only one stage of decomposition is clearly indicated in the TG curves. The residues, in nitrogen, were contaminated with carbon and hence an attempt to get an IR spectra was unsuccessful.

The benzoates of Eu, Tb and Er also decomposed to yield benzil, thus it is assumed that their mechanism of decomposition is essentially the same as that of neodymium even though the three distinct steps of decomposition were not clearly indicated in their thermal curves.

The mode of decomposition of lanthanum benzoate is believed to differ from that of neodymium benzoate in that the decomposition product, lanthanum-oxybenzoate, decomposes first to lanthanum dioxymonocarbonate and then to lanthanum trioxide and carbon dioxide in accordance with the equation
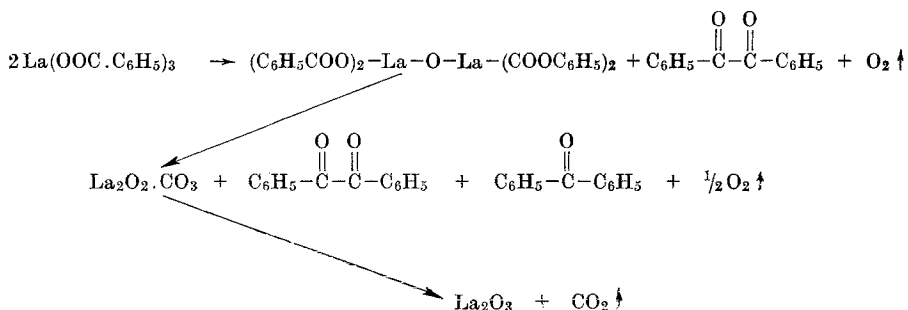
$$2\,La(OOC \cdot C_6H_5)_3 \longrightarrow (C_6H_5COO)_2-La-O-La-(COOC_6H_5)_2 + C_6H_5-\overset{O}{\overset{\|}{C}}-\overset{O}{\overset{\|}{C}}-C_6H_5 + O_2 \uparrow$$

$$La_2O_2 \cdot CO_3 + C_6H_5-\overset{O}{\overset{\|}{C}}-\overset{O}{\overset{\|}{C}}-C_6H_5 + C_6H_5-\overset{O}{\overset{\|}{C}}-C_6H_5 + {}^1\!/_2 O_2 \uparrow$$

$$La_2O_3 + CO_2 \uparrow$$

Table 13

Data for the infrared spectrum of lanthanum dioxymonocarbonate

Frequencies in cm^{-1}		
Observed	Reported [9]	Band assignment [9]
1460 − 1480	1448	Asymmetric stretching
1390	1360	
1050	1048	Symmetric stretching
845	844	out-of-plane bending
350	360	oxide

We were unable to isolate the product assumed to be benzophenone.

The second residue obtained from a TG curve of lanthanum benzoate, in vacuum, is used to obtain an IR spectrum which supports the formation of $La_2O_2 \cdot CO_3$ intermediate. The data are summarized in Table 13.

Activation energies

The activation energies calculated for these decompositions in air and vacuum are summarized in Table 14.

Table 14

Activation energies (kcal/mole) for the decomposition
of rare earth metal benzoates

Compound	Vacuum	Air
$La(COOC_6H_5)$	30.1	37.3
$Nd(COOC_6H_5)_3$	21.7	19.9
$Eu(COOC_6H_5)_3$	25.0	26.6
$Tb(COOC_6H_5)_3$	33.0	29.3
$Er(COOC_6H_5)_3$	32.2	23.3

It may be stated that the activation energies of decomposition of La, Tb and Er benzoates seems to increase in vacuum and decrease in air as the atomic number increases. The exceptions are Nd and Eu benzoates. It also appears that the activation energies of decomposition of Eu benzoate, both in vacuum and air, seem to be higher than those of Nd benzoate.

References

1. BAHOO et al., J. Indian Chem. Soc., 37 (1960) 594.
2. M. M. STEINBERG et al., J. Phys. Chem., 66 (1962) 1737.
3. V. E. PLYUSCHEV, L. M. SHKOL'NIKOVA and G. D. KUZ'NETSOVA, Dokl. Akad. Nauk USSR, 160 (1965) 366.
4. V. V. DESHPANDE and E. B. MIZRA, Proc. Chem. Symp., Chemistry and Metallurgy Comm. of the Dept. of Atomic Energy; Bhabha Atomic Research Center, Bombay-74, India, 1 (1970) 209.
5. C. V. KAVADIA and H. B. MATHUR, Indian Journal of Chemistry, 8 (1970) 638.
6. M. N. AMBROZHII and YU. A. OSIPOVA, Zh. Neorgan. Khim., 3 (1958) 2716.
7. M. D. TAYLOR, C. P. CARTER and C. I. WYNTER, J. Inorg. Nucl. Chem., 30 (1968) 1503.
8. C. J. H. SCHUTTE and K. BUIJS, Spectrochim. Acta, 20 (1964) 187.
9. J. A. GOLDSMITH and S. D. ROSS, Spectrochim. Acta, 23 A (1967) 1909.
10. N. T. MCDEVITT and N. L. BAUN, Spectrochim. Acta, 20 (1964) 799.
11. H. H. HOROWITZ and G. METZGER, Anal. Chem., 35 (1963) 1464.
12. S. R. DHARWADKAR and M. D. KARKHANAVALA, in "Thermal Analysis" Vol. 2 (Edited by R. F. Schwenker Jr. and P. D. Garn) Academic Press, New York, 1969.
13. Du Pont Thermal Analysis Manual, 1971.

RÉSUMÉ — On a étudié la décomposition des formiates et benzoates de quelques terres rares par ATD, DSC, TG et TGD. On a identifié les produits volatils ainsi que les résidus. On a calculé les énergies d'activation des décompositions et la chaleur des réactions de transition.

Les formiates des terres rares donnent comme produits de décomposition volatiles de l'anhydride carbonique et de l'eau, tandis que, dans le cas du benzoate de lanthane, on obtient du benzyle et, probablement, du benzophénone. Les autres benzoates de terres rares fournissent du diphényle comme principal produit volatil. Les trioxydes respectifs forment le résidu final.

ZUSAMMENFASSUNG — Der Verlauf der thermischen Zersetzung einiger seltener Erdmetall-Formiate und -Benzoate wurde unter Anwendung der DTA, DSC, TG und DTG-Techniken studiert. Die flüchtigen Produkte und die Rückstände wurden identifiziert. Die Aktivierungsenergien der Zersetzungsvorgänge und die Reaktionswärmen der Übergänge wurden ermittelt.

Die Zersetzung der seltenen Erdmetall-Formiate ergab Kohlendioxid und Wasser als flüchtige Produkte, während die Benzoate — im Falle von Lanthan-benzoat Benzyl und wahrscheinlich Benzophenon, im Falle anderer seltener Erdmetall-benzoate Biphenyl als flüchtige Hauptprodukte ergaben. Die entsprechenden Trioxide verblieben als Rückstand.

Резюме — Методами ДТА, ДСК, ТГ и ДТГ исследованы типы распада нескольких формиатов и бензоатов. Идентифицированы летучие продукты и остатки. Для наблюдаемых превращений рассчитаны энергии активации распада и тепловой эффект реакции.

При распаде формиатов редкоземельных металлов образуются, в качестве летучих продуктов, двуокись углерода и вода, а при распаде бензоатов — бензил и, возможно, бензофенон, в случае бензоата лантана, и дифенил, в случае бензоатов других редкоземельных металлов, — как их основные летучие продукты. Конечными продуктами в остатке являются соответствующие триокиси.